



Ga complexes of 8-hydroxyquinoline-2-carboxylic acid: Chemical speciation and biological activity

Izabela Ryza^a, Claudia Granata^b, Nadia Ribeiro^c, Edyta Nalewajko-Sieliwoniuk^a,
Andreas Kießling^d, Marta Hryniewicka^a, Winfried Plass^d, Beata Godlewska-Żyłkiewicz^a,
Sandra Cabo Verde^{c,e}, Demetrio Milea^{b,**}, Sofia Gama^{a,c,*}

^a Department of Analytical and Inorganic Chemistry, Faculty of Chemistry, University of Białystok, K. Ciołkowskiego 1K, 15-245 Białystok, Poland

^b Dipartimento di Scienze Chimiche, Biologiche, Farmaceutiche ed Ambientali, CHIBIOFARAM, Università degli Studi di Messina, V.le F. Stagno d'Alcontres, 31, 98166 Messina, Italy

^c Centro de Ciências e Tecnologias Nucleares, C2TN, Instituto Superior Técnico, Universidade de Lisboa, Estrada Nacional 10 (km 139.7), 2695-066 Bobadela LRS, Portugal

^d Institut für Anorganische und Analytische Chemie, IAAC, Friedrich Schiller Universität Jena, Humboldtstraße 8, 07743 Jena, Germany

^e Departamento de Engenharia e Ciências Nucleares, DECN, Instituto Superior Técnico, Universidade de Lisboa, 2695-066 Bobadela LRS, Portugal

ARTICLE INFO

Keywords:

Stability constants
Ga³⁺ complexes
Human microbiota
Anti-inflammatory action
Ionizing radiation

ABSTRACT

The binding ability of 8-hydroxyquinoline-2-carboxylic acid (8-HQA) towards Ga³⁺ has been investigated by ISE—H⁺ (Ion Selective Electrode, glass electrode) potentiometric and UV/Vis spectrophotometric titrations in KCl_(aq) at $I = 0.2 \text{ mol dm}^{-3}$ and at $T = 298.15 \text{ K}$. Further experiments were also performed adopting both the metal (with Fe³⁺ as competing cation) and ligand-competition approaches (with EDTA as competing ligand). Results gave evidence of the formation of the [Ga(8-HQA)]⁺, [Ga(8-HQA)(OH)]⁺, [Ga(8-HQA)(OH)₂]⁺ and [Ga(8-HQA)₂]⁺ species, the latter being so far the most stable, as also confirmed by ESI-MS analysis. Experiments were also designed to determine the stability constants of the [Ga(EDTA)]⁻ and [Ga(EDTA)(OH)]²⁻ in the above conditions. Due to the relevance of Ga³⁺ hydrolysis in aqueous systems, literature data on this topic were collected and critically analyzed, providing equations for the calculation of mononuclear Ga³⁺ hydrolysis constants at $T = 298.15 \text{ K}$, in different ionic media, in the ionic strength range $0 < I / \text{mol dm}^{-3} \leq 1.0$. The synthesis and characterization (by ElectroSpray Ionization – Mass Spectrometry (ESI-MS), Attenuated Total Reflectance - Fourier-Transform Infrared Spectroscopy (ATR-FTIR) and ThermoGravimetric Analysis (TGA)) of Ga³⁺/8-HQA complexes were also performed, identifying [Ga(8-HQA)₂]⁺ as the main isolated species, even in the solid state. Finally, the potential effects of 8-HQA and Ga³⁺/8-HQA complex towards human microbiota exposed to ionizing radiation were evaluated (namely *Actinomyces viscosus*, *Streptococcus mutans*, *Streptococcus sobrinus*, *Pseudomonas putida*, *Pseudomonas fluorescens* and *Escherichia coli*), as well as their anti-proliferative and anti-inflammatory properties. A radioprotective effect of Ga³⁺/8-HQA complex was observed on *Actinomyces viscosus*, while showing a potential radiosensitizing effect against *Streptococcus mutans* and *Streptococcus sobrinus*. No cytotoxicity on RAW264.7 murine macrophage cells was observed, neither for the free ligand or Ga³⁺/8-HQA complex. Nevertheless, Ga³⁺/8-HQA complex highlighted potential anti-inflammatory properties.

1. Introduction

Scientists are still looking for new ligands characterized by high selectivity towards metal ions and with preferable high stability constants because they could find potential applications in medicine, e.g., as

contrast-enhancing agents in diagnostic imaging, radiopharmaceuticals or chelating agents. However, their use in chelation therapy does not end with their ability to remove metals from the body. Some ligands could also play an important role in uptaking essential microelements by bacteria and some eukaryotes. An example could be siderophores,

* Corresponding author at: Centro de Ciências e Tecnologias Nucleares, C2TN, Instituto Superior Técnico, Universidade de Lisboa, Estrada Nacional 10 (km 139.7), 2695-066 Bobadela LRS, Portugal.

** Corresponding author.

E-mail addresses: dmilea@unime.it (D. Milea), sofia.gama@ctn.tecnico.ulisboa.pt (S. Gama).

<https://doi.org/10.1016/j.jinorgbio.2024.112670>

Received 4 June 2024; Received in revised form 11 July 2024; Accepted 19 July 2024

Available online 25 July 2024

0162-0134/© 2024 The Authors. Published by Elsevier Inc. This is an open access article under the CC BY-NC-ND license (<http://creativecommons.org/licenses/by-nc-nd/4.0/>).

chelating agents with a high affinity for iron, which bacteria synthesize to uptake this element from the environment [1].

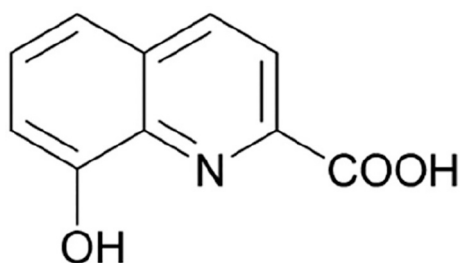
8-Hydroxyquinoline-2-carboxylic acid (8-hydroxyquinoline-2-carboxylic acid, 8-HQA) (Scheme 1) is a Tryptophan metabolite (TrpM) showing very interesting properties, such as antiproliferative and anti-migratory effects on colorectal cancer cells [2]. Furthermore, is one of the products of the so-called kynurenine pathway [3], which is related to the immune system through the inflammatory response [4]. 8-HQA was also recently recognized as a siderophore and identified in high concentrations ($0.5\text{--}5.0 \times 10^{-3} \text{ mol dm}^{-3}$) in the digestive tract (gut) of several Noctuid larvae and other lepidopterans [3].

Studies have shown that, in insects, iron and other microelements are absorbed in the digestive tract, and more precisely in the gut, through microorganisms that create a rich and complex microflora community [5,6]. Moreover, it was found that the amount of iron in the diet of insects directly impacts the population of microflora in their gut [5]. Gama et al. [7] investigated the chelation properties of 8-HQA towards Fe^{2+} and Fe^{3+} and the thermodynamic study of the complexes has shown that 8-HQA may act as a natural chelator for iron ions and may be potentially used to regulate the intestinal microbiota or act as an antimicrobial agent.

Iron is an essential microelement, crucial for the growth of all organisms, including bacteria. Interestingly, when an iron-dependent process needs to be interrupted or inhibited, Ga^{3+} cation can be used [8,9]. An example is the “Trojan horse” approach described in the literature as an antimicrobial strategy, which relies in “tricking” bacteria so that they take up a metal resembling Fe^{3+} , but toxic, which cannot effectively replace it in the cell [10]. This may result into the failure of fundamental biological processes, either due to lack of iron or to the toxicity of the uptaken metal, and the consequent cell death. For example, exposure to gallium may inhibit bacterial growth and biofilm formation [9].

Since the 1970s, the mimicry between gallium and ferric iron has been deeply investigated. The general coordination chemistry of Ga^{3+} and Fe^{3+} is quite similar. This includes their charge (+3), ionic radius ($\text{Ga}^{3+} \sim 0.62 \text{ \AA}$, $\text{Fe}^{3+} \sim 0.65 \text{ \AA}$ [8–11]), coordination number (six) [11]. Both cations undergo comparable reactions in aqueous solution as both of them are strong Lewis acids. This is also valid when considering hydrolytic processes, which deeply affect the speciation of the systems. Due to all the mentioned points, Ga^{3+} usually presents similar binding abilities as Fe^{3+} , including binding with macromolecular components of serum, e.g., transferrin, albumin and globulins [12,13] or with siderophores, e.g. pyochelin [14]. Furthermore, gallium’s relevance in biology and medicine is also related to the fact that ^{67}Ga and ^{68}Ga complexes are used as radiotracers in nuclear medicine for diagnostic imaging procedures [11]. Several gallium radiopharmaceuticals are already used worldwide for imaging of tumor cells, multiple types of cancer, heart diseases, and even brain disorders, as well as infection radiotracers. For the latest, $^{67/68}\text{Ga}$ -siderophores are being exploited [15–22].

Due to the proven action of 8-HQA as a siderophore [7], and following our previous studies on this metal chelator, its evaluation as Ga^{3+} chelating agent is worth of investigation. This paper presents the



Scheme 1. Structure of 8-hydroxyquinoline-2-carboxylic acid (8-HQA)

results of research, based on a multi-technique approach [23], aimed at obtaining a comprehensive set of information necessary to assess the chemical speciation of the $\text{Ga}^{3+}/8\text{-HQA}$ system.

As such, the binding ability of 8-HQA towards Ga^{3+} has been investigated by ISE- H^+ (Ion Selective Electrode, glass electrode) potentiometric and UV/Vis spectrophotometric titrations in $\text{KCl}_{(\text{aq})}$ at $I = 0.2 \text{ mol dm}^{-3}$ and at $T = 298.15 \text{ K}$. The data obtained from ISE- H^+ potentiometric titrations were supported by the results acquired by the application of both the metal (with Fe^{3+} as competing cation) and ligand-competition approaches (with EDTA as competing ligand) [24–27]. The latter also allowed a more thorough investigation of the $\text{Ga}^{3+}/\text{EDTA}$ system under the experimental conditions given above, typically used in biological studies, providing an accurate dataset of stability constants for the $\text{Ga}_p(\text{EDTA})_q\text{H}_r$ species.

Considering the importance of Ga^{3+} acid-base properties for its solution behavior, a critical literature data analysis on its hydrolysis has also been performed, providing all the tools necessary to calculate its hydrolysis constants at $T = 298.15 \text{ K}$ in different ionic media in the ionic strength range $0 < I / \text{mol dm}^{-3} \leq 1.0$.

Besides the studies performed in aqueous solution, $\text{Ga}^{3+}/8\text{-HQA}$ complexes were also synthesized and fully characterized by ESI-MS (electrospray ionization mass spectrometry), ATR-FTIR (attenuated total reflectance-Fourier transform infrared) spectroscopy, and TGA (thermogravimetric analysis).

Finally, considering the above-cited importance of both 8-HQA and Ga^{3+} from a biological and medical point of view, some tests were also performed to investigate the anti-proliferative and anti-inflammatory properties of 8-HQA and its Ga^{3+} complexes, as well as their potential protective effect on human microbiota exposed to ionizing radiation. This can be particularly important to our study as it is demonstrated that the human gut microbiome plays a role in the development of radiation resistance in cancer patients under radiotherapy treatment [28].

2. Experimental

2.1. Chemicals

8-hydroxyquinoline-2-carboxylic acid (8-HQA) solutions were prepared by weighting the pure compound. A minimum known amount of ethanol ($\text{EtOH} < 2.0\% \text{ v/v}$) was used to promote initial ligand solubilization in water. Ethylenediaminetetraacetic acid (EDTA) standard solutions were prepared from the $\text{Na}_2\text{H}_2\text{EDTA} \cdot 2\text{H}_2\text{O}$ salt and standardized against calcium carbonate, previously dried in an oven at $T = 383.15 \text{ K}$ for at least 2 h. Ga^{3+} and Fe^{3+} solutions were prepared from their salts, $\text{GaNO}_3 \cdot x\text{H}_2\text{O}$ and $\text{FeCl}_3 \cdot 6\text{H}_2\text{O}$ respectively, and standardized against EDTA [29]. Potassium chloride aqueous solutions were prepared by weighting the pure salt, previously dried in an oven at $T = 383.15 \text{ K}$ for at least 2 h. HCl and KOH solutions were prepared by diluting concentrated ampoules and were standardized against tris(hydroxymethyl)aminomethane and potassium hydrogen phthalate, respectively, previously dried in an oven at $T = 383.15 \text{ K}$ overnight. KOH solutions were kept in dark, plastic bottles and preserved from atmospheric CO_2 by means of soda lime traps. All solutions were prepared using grade A glassware and analytical grade water ($R = 18 \text{ M}\Omega \text{ cm}^{-1}$) and were used immediately after preparation. For the synthesis of $\text{Ga}^{3+}/8\text{-HQA}$ complexes, MeOH was also used as solvent, triethylamine (Et_3N) to adjust pH, and diethyl ether (Et_2O) during purification. All chemicals and solvents were purchased from Sigma-Aldrich (Europe) and its sub-brands at the highest available purity.

2.2. Apparatus and procedure for potentiometric measurements

The potentiometric apparatus consisted of two Thermo Scientific™ Orion Star™ T910 pH titrators, equipped with Orion 8102BNUWP ROSS Ultra Combination glass electrodes. The Orion Star T900 Series Titrator software (version V3.4.0) was used to control all the parameters of

automatic titration, the titrant delivery, data acquisition and e.m.f. stability. The estimated precision was ± 0.2 mV and 0.005 cm^3 for the e. m.f. and titrant volume readings, respectively. Potentiometric titrations were performed at $T = 298.15 \pm 0.1$ K in thermostatted cells under magnetic stirring. Purified Ar gas was bubbled through the solution to exclude O_2 and CO_2 . Due to the expected high stability of the $\text{Ga}^{3+}/8\text{-HQA}$ complexes, the ligand-competition approach was additionally applied, using EDTA as competing ligand. The titrand solutions consisted of different amounts of 8-HQA ($0.9 \leq c_L / \text{mmol dm}^{-3} \leq 1.3$), EDTA ($0 \leq c_L / \text{mmol dm}^{-3} \leq 1.0$), metal cation ($0.9 \leq c_{\text{Ga}} / \text{mmol dm}^{-3} \leq 1.3$), HCl ($3.9 \leq c_{\text{H}} / \text{mmol dm}^{-3} \leq 5.2$), and $\text{KCl}_{(\text{aq})}$ to reach an ionic strength of $I = 0.2 \text{ mol dm}^{-3}$.

Since the stability of analogous $\text{Fe}^{3+}/8\text{-HQA}$ complexes is already known exactly in the same conditions as the system under study, some measurements were also performed according to the cation competition approach [30]. To this aim, titrand solutions consisted of 8-HQA ($1.0 \leq c_L / \text{mmol dm}^{-3} \leq 1.2$), Fe^{3+} ($0.4 \leq c_{\text{Fe}} / \text{mmol dm}^{-3} \leq 1.1$), Ga^{3+} ($0.4 \leq c_{\text{Ga}} / \text{mmol dm}^{-3} \leq 1.1$), HCl ($2.0 \leq c_{\text{H}} / \text{mmol dm}^{-3} \leq 3.6$), and $\text{KCl}_{(\text{aq})}$ to reach an ionic strength of $I = 0.2 \text{ mol dm}^{-3}$.

Solutions were prepared in 50 cm^3 volumetric flasks. Measurements were performed considering different concentration ratios of ligands and metals. Further experimental details are reported in Table S1. For each of those ratios, at least two potentiometric titrations were performed, applying minor changes in the concentrations of reactants. Potentiometric measurements were carried out by titrating 25 cm^3 of the titrand solution with standard KOH solutions up to the observation of a precipitate formation ($\text{pH} \sim 7.0\text{--}7.5$). If precipitation was not observed, measurements were stopped at $\text{pH} \sim 10.5\text{--}11.0$. Before each experiment, independent titrations of HCl with standard KOH were performed to calibrate the electrode under the same medium and ionic strength conditions as the investigated systems, determining the electrode potential (E^0) and the acidic junction coefficient (j_a). By this procedure, the pH scale used is the free scale, $\text{pH} = -\log[\text{H}^+]$, where $[\text{H}^+]$ sets for the free proton concentration (not activity). The reliability of the electrode calibration in the alkaline pH was checked by determining $\text{p}K_w$ values, which resulted in $\text{p}K_w = 13.76 \pm 0.02$ (\pm standard deviation). During each titration, around 80–100 data points were collected, and the equilibrium state during titrations was checked by adopting the usual precautions, i.e., checking the time required to reach equilibrium and performing back titrations.

2.3. Apparatus and procedure for UV/Vis spectrophotometric measurements

Spectrophotometric titrations were carried out using a double-beam Thermo Scientific EVOLUTION One Plus UV/Vis spectrophotometer equipped with quartz cuvette with a fixed 1 cm path length. Data of absorbance vs. wavelength (λ / nm) were collected by the Insight™ Pro (version 3.0.0.109) software. Measurements were performed in a thermostatted cell at $T = 298.15 \pm 0.1$ K in the $200 \leq \lambda / \text{nm} \leq 800$ wavelength range. E.m.f. measurements and titrant additions were made using the previously described potentiometric equipment. When the solution in the cell was titrated by a competing cation solution, it was added to the cell by Eppendorf Research® plus single-channel pipette with variable volume setting ($20\text{--}200 \text{ mm}^3$). Solutions were kept under magnetic stirring and Ar gas was bubbled to avoid the presence of $\text{CO}_{2(\text{g})}$ and $\text{O}_{2(\text{g})}$ in samples.

UV/Vis spectrophotometric measurements were carried out by titrating 30 cm^3 of the titrand solution with standard KOH solution, up to $\text{pH} \sim 10.5\text{--}11.0$. The measured solutions consisted of different amounts of 8-HQA ($0.02 \leq c_L / \text{mmol dm}^{-3} \leq 0.33$), Fe^{3+} ($0 \leq c_{\text{Fe}} / \text{mmol dm}^{-3} \leq 0.20$), Ga^{3+} ($0 \leq c_{\text{Ga}} / \text{mmol dm}^{-3} \leq 0.20$), HCl ($0.39 \leq c_{\text{H}} / \text{mmol dm}^{-3} \leq 11.00$), and $\text{KCl}_{(\text{aq})}$ to reach the pre-established ionic strength of $I = 0.2 \text{ mol dm}^{-3}$, in suitable concentrations to achieve desired molar ratios (reported in Table S2). During each titration ca. 30–45 data points were collected, along with recorded spectra. Metal

competition UV/Vis spectrophotometric measurements were also done, by titrating $\text{Ga}^{3+}/8\text{-HQA}$ solutions at a fixed $\text{pH} \sim 3.5\text{--}4.0$ with Fe^{3+} , and *vice versa* (see Table S2).

2.4. Apparatus and procedure for ESI-MS measurements of aqueous samples

ESI-MS measurements of aqueous samples were carried out using an ESI-LC-MS/MS system (Shimadzu 8040, Japan), equipped with a LC-30 CE pump and a SIL-30 AC autosampler. Nebulizing gas (N_2) flow was $3 \text{ dm}^3 \text{ min}^{-1}$, drying gas (N_2) flow was $15 \text{ dm}^3 \text{ min}^{-1}$, desolvation line (DL) temperature $T = 493.15$ K, heat block temperature $T = 503.15$ K. Elution was in isocratic mode with the mobile phase consisting of: A: MeOH (95%), B: HCOOH in H_2O (5%), scanning mode (ESI+ and ESI-), flow of mobile phase: $0.3 \text{ cm}^3 \text{ min}^{-1}$, sample volume: 5 mm^3 . Analyzed aqueous solutions consisted of different amounts of 8-HQA and Ga^{3+} in suitable concentrations to reach the desired concentration ratios ($1:1 \leq c_{8\text{-HQA}}:c_{\text{Ga}} \leq 3:1$), EtOH at 2% v/v and HCl or KOH to adjust pH (4, 7 and 10). Samples were freshly prepared and injected immediately after preparation.

2.5. Synthesis and characterization of $\text{Ga}^{3+}/8\text{-HQA}$ metal complexes

The synthesis of 8-HQA metal complexes was performed in MeOH in two variants: a) with, and b) without the addition of Et_3N . Three aliquots of 8-HQA ($\sim 50 \text{ mg}$) were placed in Erlenmeyer flasks (50 cm^3), followed by the addition of MeOH (20 cm^3), with and without the addition of Et_3N (0.5 cm^3). The mixtures were placed on a magnetic stirrer and covered with parafilm to restrain MeOH evaporation. The solutions were left on the magnetic stirrer until the complete dissolution of 8-HQA, after which Ga^{3+} solution was added. Three aliquots of Ga (NO_3) $_3 \cdot x\text{H}_2\text{O}$ ($x = 7.6$ according to TGA measurements, using a Netzsch STA 409 PC/PG, data not shown) were accurately weighted and dissolved in MeOH (5 cm^3). The metal salt was not easily dissolved in MeOH, so metal suspensions prepared this way were quantitatively added to the ligand solution and the mixtures were closed with parafilm and left stirring overnight. The mass of metal salt was strictly dependent on the mass of the weighted ligand, to achieve three different molar ratios ($1:1 \leq n_{8\text{-HQA}}:n_{\text{Ga}} \leq 3:1$). On the next day, the solutions were put off the magnetic stirrer and divided into two further aliquots. The first part was left in the Erlenmeyer flasks covered with riddled parafilm and put under the crystallization hood. The second part of the solutions was left in the fridge (at $T = 278.15$ K). Both solutions were kept under strict observation, focusing on signs of crystallization. The pH of the samples was checked with a pH-meter and its value was always around 10, ensuring that 8-HQA was in its fully deprotonated form [31]. All the steps were repeated as described above for the system without addition of Et_3N , except for the addition of the base itself. In this system pH value was always around 4.

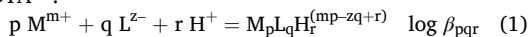
The obtained precipitates were characterized by ATR-FTIR, ESI-MS and TGA. The acquisition of the IR spectra was carried out using a Bruker Vertex 70 with a Specac Golden Gate ATR bridge and the data obtained were processed by OPUS software. Further characterization was pursued by TGA and the thermogravimetric curves were recorded using a Netzsch STA 409 PC/PG. For ESI-MS measurements (ESI+ and ESI-), isolated precipitates were re-dissolved in MeOH. The apparatus was a Bruker maXis impact (QTOF) Mass Spectrometer, coupled to a Thermo Ultimate 3000 quaternary UHPLC system with autosampler, double column changer and DAD (diode array detector). Nebulizing gas was N_2 .

2.6. Thermodynamic calculations and potentiometric and spectrophotometric data analysis

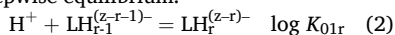
Experimental data from the potentiometric titrations were analyzed by the BSTAC [32] computer program, to determine the electrode

calibration parameters (i.e., K_{ws} , E^0 and j_a), as well as the stability constants of the species determined. Similarly, experimental spectrophotometric data were analyzed by the HypSpec program from the Hyperquad suite [33]. Noteworthy, both the procedures allowed by HypSpec were followed: i.e., reporting spectra as a function of pH (read after equilibrium reached after each base addition, and before the recording of each spectrum) or directly using total c_H as input (not pH). The distribution diagrams were then obtained by the PyES program [34].

Within the manuscript, if not differently specified, the hydrolysis constants of Ga^{3+} ($q = 0, r < 0$), the protonation constants of the ligands ($L^{z-}, p = 0$) and the complex formation constants are given according to the overall equilibrium, with $M^{m+} = Fe^{3+}$ or Ga^{3+} and $L^{z-} = 8-HQA^{2-}$ or $EDTA^{4-}$:



Ligands protonation constants may also be given according to the stepwise equilibrium:



Protonation, hydrolysis and complex formation constants, concentrations and ionic strengths are expressed in the molar (c , mol dm^{-3}) concentration scale. Errors are reported as \pm standard deviation. Where not strictly relevant, charges of various species are omitted for simplicity.

2.7. Microbial susceptibility assays

The ligands were weighted and solubilized in MilliQ-H₂O under alkaline pH (using 0.1 mol dm^{-3} KOH solution). For the 2:1 ligand-to-metal complexes, a known amount of the solution of the corresponding metal salt was added, and the final pH of the solutions was adjusted to $\sim 7-8$. The bacterial isolates used in this study were representatives of the oral cavity (*Actinomyces viscosus*, *Streptococcus mutans* and *Streptococcus sobrinus* from clinical isolates), and the gut microbiota (*Pseudomonas putida* ATCC12633, *Pseudomonas fluorescens* ATCC 13525 and *Escherichia coli* ATCC 8739). The susceptibility assessment of the compounds towards each bacteria was accomplished by the disk diffusion method [35]. Briefly, a bacterial suspension of 10^6 cells cm^{-3} was inoculated onto Tryptone Soya Agar (TSA, Oxoid Ltd., Basingstoke, UK) plates (one plate *per* concentration of the compound to be tested). An aliquot of 10 mm^3 of compounds at concentration of 6 mg cm^{-3} , 3 mg cm^{-3} and 1.5 mg cm^{-3} was soaked on sterile filter disks (6 mm) and distributed on the surface of TSA plates. As controls, the same volume of the metal salt solution, Milli-Q water and Streptomycin solution (100 μg cm^{-3} , Hyclone, Cytiva, UT, USA) were applied in the disks. The plates were incubated for 48 h at $T = 310.15$ K. The diameter of inhibition zone (around each filter disk) was measured using a caliper.

2.8. Irradiation experiments and microbial inactivation studies

A Co-60 experimental chamber (Precisa 22, Graviner Manufacturing Company Ltd., UK) was used for samples irradiation. During the irradiation procedure, the sample vials (1 cm^3) were placed in a rotating support positioned inside the chamber at 19.0 cm depth and 26.0 cm height, allowing absorbed dose uniformity. The dose rate was 0.6 kGy h^{-1} , and the doses absorbed by the samples (0.17–0.53 kGy) were estimated using routine Perspex dosimeter (Harwell Company, Didcot, Oxfordshire, UK). The microbial inactivation studies were performed using bacterial suspensions (10^6 cells cm^{-3}) in physiological serum (0.9% NaCl) and in compounds solutions at 1 mg cm^{-3} . The microbial inactivation kinetics was assessed in four substrates (physiological serum, 8-HQA, $[Ga(8-HQA)_2]^-$, and $Ga(NO_3)_3$) to evaluate the effect of ligand and its complex on the bacterial isolates radioresistance. The number of viable bacterial cells in non-irradiated and irradiated samples was estimated using the direct plating method by inoculation in triplicate of aliquots of serial decimal dilutions onto TSA. The inoculated Petri dishes were incubated at $T = 310.15$ K during seven days, and the results

were expressed as logarithm of Colony Forming Units *per* cm^3 (log CFU cm^{-3}). Non-irradiated suspensions in the same substrates followed all the experiments and were used as controls and termed as 0 kGy. The D_{10} values for each bacterial isolate in each substrate, representing the dose required for 90% inactivation of the initial bacterial population, were determined as the negative reciprocal of the slope of the survival curve (log CFU cm^{-3} vs. absorbed dose) [36]. When possible, three independent irradiation batches were performed.

2.9. Anti-proliferative and anti-inflammatory assays

The effects of compounds solutions on cell viability were assessed by the anti-proliferative WST-1 assay using the murine monocyte macrophage RAW264.7 cell line (TIB-71™). This assay is based on the cleavage of the tetrazolium salt WST-1 to formazan by cellular mitochondrial dehydrogenases [37]. Compounds' solutions were prepared in sterile ultra-pure water and filtered, with the concentrations to be tested as 100 μmol dm^{-3} , 10 μmol dm^{-3} , 1 μmol dm^{-3} , and 0.1 μmol dm^{-3} . Briefly, RAW 264.7 cells were seeded at a density of 1.0×10^5 cells/well in 96-well plates in Dulbecco's modified eagle medium (DMEM) supplemented with 10% fetal bovine serum (FBS) and incubated at $T = 310.15$ K and 5% CO₂ for 24 h. The culture media was removed, and the cellular monolayer was washed twice with phosphate-buffered saline (PBS) solution. After removal of the PBS, 100 mm^3 of minimum essential media (MEM) $2 \times$ supplemented with 2% FBS, and 100 mm^3 of the prepared samples were added to each well, and the plates were incubated for 24 h at $T = 310.15$ K, 5% CO₂ conditions. The inoculum was removed from the wells and 100 mm^3 of DMEM 10% FBS and 10 mm^3 of WST-1 (Roche, Switzerland) were added to each well. Cells were incubated for 6 h under the same conditions. The absorbance at $\lambda = 450$ nm was measured using a $\lambda = 620$ nm reference wavelength, on a microplate reader (EZ Read 800, Biochrom, Cambridge UK). The cell viability was determined as the percentage of the average absorbance resulting from triplicate runs of treated cells relative to untreated control cells, with absorbances of corresponding controls subtracted to address possible matrix interferences, using the following equation:

$$\% \text{cell viability} = \frac{\text{treated cells} - \text{culture medium}}{\text{untreated cells} - \text{culture medium}} \times 100 \quad (3)$$

To test the anti-inflammatory activity, the Griess assay was used, which is an *in vitro* test that uses the RAW264.7 cells to generate the pro-inflammatory molecule nitric oxide (NO) [38]. It consists of a two-step diazotization reaction based on the reaction of NO_2^- with sulphanilamide and *N*-(1-naphthyl)ethylene-diamine, which generates a purple-azo-dye product that can be spectrophotometrically monitored at $\lambda = 540$ nm [39]. RAW264.7 cells were seeded at a density of 1.0×10^5 cells / well in a 96-well plate in DMEM supplemented with 10% FBS and incubated at $T = 310.15$ K and 5% CO₂ for 24 h. The culture media were removed, and cells washed with PBS and incubated for 4 h at $T = 310.15$ K and 5% CO₂ with different concentrations of 8-HQA (0.25–2.5 mmol dm^{-3}) and $[Ga(8-HQA)_2]^-$ (0.3–2.4 mmol dm^{-3}). After removal of the compounds' solutions, the cells were stimulated with 0.5 μg cm^{-3} of lipopolysaccharide (LPS, from *Escherichia coli*) for 20 h. The supernatant was transferred to a new 96-well plate and Nitrite Assay kit (Griess reagent; MAK367, Sigma-Aldrich) was used to determine nitrite concentration, following manufacturer instructions. The absorbance at $\lambda = 540$ nm was measured at room temperature using the same microplate reader. The concentration of nitrite in control and test samples was determined from a sodium nitrite standard curve performed according to the assay kit. Experiments were carried out in triplicate. The % of inhibition of nitrite production was estimated as expressed in the equation:

$$\text{Inhibition (\%)} = \frac{\text{Control} - \text{Test}}{\text{Control}} \times 100 \quad (4)$$

in which *Control* is the nitrite concentration of the control (from untreated cells in culture media), while *Test* is the nitrite concentration of test samples.

2.10. Statistical analysis on biological tests

Results were expressed as mean \pm standard deviation. For both the irradiation experiments and microbial inactivation studies and the anti-proliferative and anti-inflammatory assays, the differences among substrates were analyzed using the one-way analysis of variance (ANOVA) followed by Tukey's HSD test with $\alpha = 0.05$.

3. Results and discussion

3.1. Chemical speciation studies in aqueous solution

3.1.1. Acid-base behavior of cations and ligands

For an accurate speciation study, it is necessary to know the acid-base properties of all the elements involved in the complexation (8-HQA, EDTA, Fe^{3+} and Ga^{3+}) in the exact conditions of the experiments. Protonation and hydrolysis constants of 8-HQA, EDTA and Fe^{3+} at $T = 298.15$ K and $I = 0.2$ mol dm^{-3} were taken from previous work and are reported in Table 1 together with other constants used in the speciation model [7,31]. Concerning spectrophotometric measurements, the specific molar absorbances of 8-HQA and its protonated species were re-determined in the same experimental conditions of this work (spectra in Fig. S1 in the wavelength range $200 \leq \lambda / \text{nm} \leq 500$).

Concerning Ga^{3+} hydrolysis, the analysis of main stability constants databases [40–42], as well as specific collections dedicated to the hydrolysis of metal cations [43], revealed wide discrepancies in both the nature of species formed and their stability, as also detailed by Baes and Mesmer [44] and Brown and Ekberg [45]. For this reason, we decided to perform a comprehensive literature data analysis to obtain some reliable values, at least for the main species. To this aim, all main publications reporting hydrolysis constants and solubility products of Ga^{3+} in aqueous ionic media at different ionic strengths and temperatures were collected and critically analyzed together with data already present in the above databases and collections [40–45]. Available data allowed the modelling of the dependence on medium and ionic strength of only the four mononuclear species (*i.e.*, $[\text{Ga}(\text{OH})]^{2+}$, $[\text{Ga}(\text{OH})_2]^+$, $[\text{Ga}(\text{OH})_3(\text{aq})]$

Table 1

Stability constants of species included in the speciation model for data analysis, at $I = 0.2$ mol dm^{-3} in $\text{KCl}(\text{aq})$ and $T = 298.15$ K.

Equilibrium	$\log \beta_{\text{pqr}}$
OH^-	$-13.76 \pm 0.02^{\text{a, b}}$
$8\text{-HQA}^{2-} + \text{H}^+ = (\text{8-HQA})\text{H}^-$	9.562 ^c
$8\text{-HQA}^{2-} + 2\text{H}^+ = (\text{8-HQA})\text{H}_2$	13.520 ^c
$\text{EDTA}^{4-} + \text{H}^+ = (\text{EDTA})\text{H}^{3-}$	9.354 ^c
$\text{EDTA}^{4-} + 2\text{H}^+ = (\text{EDTA})\text{H}_2^{2-}$	15.447 ^c
$\text{EDTA}^{4-} + 3\text{H}^+ = (\text{EDTA})\text{H}_3$	18.160 ^c
$\text{EDTA}^{4-} + 4\text{H}^+ = (\text{EDTA})\text{H}_4$	20.304 ^c
$\text{Ga}^{3+} + \text{H}_2\text{O} = \text{Ga}(\text{OH})^{2+} + \text{H}^+$	-3.41 ^b
$\text{Ga}^{3+} + 2\text{H}_2\text{O} = \text{Ga}(\text{OH})_2^+ + 2\text{H}^+$	-7.15 ^b
$\text{Ga}^{3+} + 3\text{H}_2\text{O} = \text{Ga}(\text{OH})_3 + 3\text{H}^+$	-10.69 ^b
$\text{Ga}^{3+} + 4\text{H}_2\text{O} = \text{Ga}(\text{OH})_4 + 4\text{H}^+$	-16.78 ^b
$\text{Fe}^{3+} + \text{H}_2\text{O} = \text{Fe}(\text{OH})^{2+} + \text{H}^+$	-2.27 ^c
$\text{Fe}^{3+} + 2\text{H}_2\text{O} = \text{Fe}(\text{OH})_2^+ + 2\text{H}^+$	-6.40 ^c
$\text{Fe}^{3+} + 3\text{H}_2\text{O} = \text{Fe}(\text{OH})_3 + 3\text{H}^+$	-14.36 ^c
$\text{Fe}^{3+} + 4\text{H}_2\text{O} = \text{Fe}(\text{OH})_4 + 4\text{H}^+$	-22.71 ^c
$2\text{Fe}^{3+} + 2\text{H}_2\text{O} = \text{Fe}_2(\text{OH})_2^{4+} + 2\text{H}^+$	-2.86 ^c
$3\text{Fe}^{3+} + 4\text{H}_2\text{O} = \text{Fe}_3(\text{OH})_4^{5+} + 4\text{H}^+$	-5.98 ^c
$\text{Fe}^{3+} + 8\text{-HQA}^{2-} + \text{H}^+ = [\text{Fe}(\text{8-HQA})\text{H}]^{2+}$	16.14 ^c
$\text{Fe}^{3+} + 8\text{-HQA}^{2-} = [\text{Fe}(\text{8-HQA})]^{+}$	13.9 ^c
$\text{Fe}^{3+} + 8\text{-HQA}^{2-} = [\text{Fe}(\text{8-HQA})(\text{OH})] + \text{H}^+$	11.58 ^c
$\text{Fe}^{3+} + 8\text{-HQA}^{2-} = [\text{Fe}(\text{8-HQA})(\text{OH})_2]^- + 2\text{H}^+$	3.67 ^c
$\text{Fe}^{3+} + 2\text{8-HQA}^{2-} = [\text{Fe}(\text{8-HQA})_2]^-$	26.95 ^c

^a value obtained from electrode calibrations, \pm standard deviation; ^b this work; ^c from ref. [7].

and $[\text{Ga}(\text{OH})_4]^-$) at $T = 298.15$ K, but not the simultaneous modelling of the temperature dependence. In fact, available data at variable temperatures were mainly obtained at infinite dilution or single ionic strengths, thus not ensuring sufficient variability for a comprehensive data treatment. Collected data (hydrolysis constants of $[\text{Ga}(\text{OH})_r]^{(3-r)}$ species, with $1 \leq r \leq 4$, are reported in Tables S3-S6), as well as the detailed description of both the model used (*i.e.*, the so-called *Pure Water Model* [34]) and results obtained (Table S7), are reported as supplementary information. Here we just report, in Table 1, the hydrolysis constants calculated in chloride media at $I = 0.2$ mol dm^{-3} and $T = 298.15$ K (*i.e.*, those used in this work). Worth mentioning here is also the fact that a global analysis revealed the lack of systematic studies on Ga^{3+} acid-base properties, highlighting the necessity of further dedicated experimental studies. This is particularly relevant, for example, for the values relative to $[\text{Ga}(\text{OH})_4]^-$ species, which is probably overestimated, due to its formation upon redissolution of the sparingly soluble $[\text{Ga}(\text{OH})_3(\text{s})]$ at alkaline pH. From our experience, this phenomenon is quite common for results obtained during solution studies for species formed immediately before or after the formation of solid species, since precipitation, if not immediately identified during experiments, results in the overestimation of the stability of those species in successive data analysis. Considering that, it is also important to emphasize that stability constants obtained, also in this work, are affected, and strictly dependent, on the values of other constants used in models: though the speciation (in terms of relative formation percentages of various species) of a studied system should be unaltered and only determined by experiments, the values of the constants obtained numerically depend on "numbers" used as input. As such, self-consistency of stability constants datasets is essential to obtain reliable speciation models.

3.1.2. Formation and stability of $\text{Ga}^{3+}/8\text{-HQA}$ species

The formation and stability of the $\text{Ga}^{3+}/8\text{-HQA}$ species was determined through potentiometric measurements under various conditions (see Table S1). Due to the expected high stability of the species formed, further measurements using EDTA or Fe^{3+} as competing ligand and metal, respectively, were also performed. Noteworthy, due to the system's complexity, all measurements detailed in Table S1 were analyzed together, to maximize the variability of the conditions and to reduce any systematic errors. This approach unavoidably increased the level of uncertainty of the system, leading to higher errors associated with the refined parameters (*i.e.*, stability constants and overall quality-of-fit parameters, *e.g.*, standard and mean deviations), but led to more reliable results. As such, the file for data analysis by BSTAC [32] software consisted of all measurements performed as reported in Table S1, thus including as input also the species formed by EDTA (*i.e.*, protonation constants) and Fe^{3+} (*i.e.*, its hydrolysis and stability constants of $\text{Fe}^{3+}/8\text{-HQA}$ complexes), as reported in Table 1. Like that, the only adjustable parameters were the stability constants of both $\text{Ga}^{3+}/8\text{-HQA}$ and $\text{Ga}^{3+}/\text{EDTA}$ complexes, as detailed below. Concerning the latter, it is worth mentioning that their stability constants were determined here for the first time in the exact conditions of this work.

Noteworthy, the stability constants of $\text{Fe}^{3+}/\text{EDTA}$ complexes were not considered, since there were no titrations in which Fe^{3+} and EDTA were simultaneously present. The overall data analysis was performed considering the possible formation of species similar to those of the analogous $\text{Fe}^{3+}/8\text{-HQA}$ system (*i.e.*, $[\text{Ga}(\text{8-HQA})\text{H}]^{2+}$, $[\text{Ga}(\text{8-HQA})]^{+}$, $[\text{Ga}(\text{8-HQA})(\text{OH})]$, $[\text{Ga}(\text{8-HQA})(\text{OH})_2]^-$, $[\text{Ga}(\text{8-HQA})_2]^-$ and $[\text{Ga}(\text{8-HQA})_3]^{3-}$). The best model was that considering the formation of only the $[\text{Ga}(\text{8-HQA})]^{+}$, $[\text{Ga}(\text{8-HQA})(\text{OH})]$, $[\text{Ga}(\text{8-HQA})(\text{OH})_2]^-$ and $[\text{Ga}(\text{8-HQA})_2]^-$ species, whose stability constants are reported in Table 2, together with those obtained also for $\text{Ga}^{3+}/\text{EDTA}$ complexes, namely $[\text{Ga}(\text{EDTA})]^-$ and $[\text{Ga}(\text{EDTA})(\text{OH})]^{2-}$. The determination of the stability constants of these two species was possible because, as EDTA competes with 8-HQA towards Ga^{3+} complexation, it also works the other way round. Further discussion of this topic follows. As observed in the speciation diagram of $\text{Ga}^{3+}/8\text{-HQA}$ system (Fig. 1), the main species

Table 2

Stability constants of $\text{Ga}_p(\text{8-HQA})_q\text{H}_r$ and $\text{Ga}_p(\text{EDTA})_q\text{H}_r$ species at $I = 0.2 \text{ mol dm}^{-3}$ in $\text{KCl}_{(\text{aq})}$ and $T = 298.15 \text{ K}$.

Equilibrium	$\log \beta_{\text{pqr}}^a$
$\text{Ga}^{3+} + 8\text{-HQA}^{2-} = [\text{Ga}(\text{8-HQA})]^+$	13.18 ± 0.03
$\text{Ga}^{3+} + 8\text{-HQA}^{2-} = [\text{Ga}(\text{8-HQA})(\text{OH})] + \text{H}^+$	9.13 ± 0.08
$\text{Ga}^{3+} + 8\text{-HQA}^{2-} = [\text{Ga}(\text{8-HQA})(\text{OH})_2]^- + 2\text{H}^+$	4.78 ± 0.04
$\text{Ga}^{3+} + 2 \text{8-HQA}^{2-} = [\text{Ga}(\text{8-HQA})_2]^-$	26.04 ± 0.02
$\text{Ga}^{3+} + \text{EDTA}^{4-} = [\text{Ga}(\text{EDTA})]^-$	20.22 ± 0.04
$\text{Ga}^{3+} + \text{EDTA}^{4-} = [\text{Ga}(\text{EDTA})(\text{OH})]^{2-} + \text{H}^+$	14.70 ± 0.03

^a \pm standard deviation.

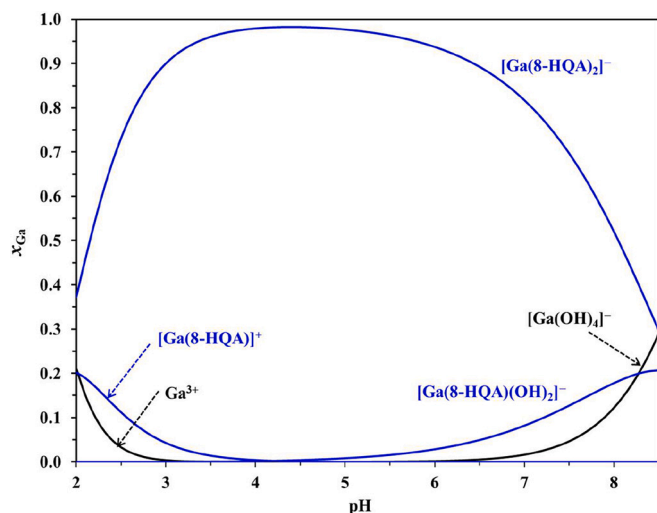


Fig. 1. Distribution diagram of $\text{Ga}_p(\text{8-HQA})_q\text{H}_r$ species as a function of pH. $c_{\text{8-HQA}} = 1 \times 10^{-3} \text{ mol dm}^{-3}$, $c_{\text{Ga}} = 0.5 \times 10^{-3} \text{ mol dm}^{-3}$.

over a wide pH range is $[\text{Ga}(\text{8-HQA})_2]^-$. The formation of other species is highly dependent on the applied $c_{\text{L}}:c_{\text{M}}$ ratios.

The analysis of spectrophotometric data proved the formation of three species, namely $[\text{Ga}(\text{8-HQA})]^+$, $[\text{Ga}(\text{8-HQA})(\text{OH})_2]^-$ and $[\text{Ga}(\text{8-HQA})_2]^-$. It was not possible to determine the stability constant of the $[\text{Ga}(\text{8-HQA})(\text{OH})]$ species since its formation percentage was too low in the conditions of spectrophotometric measurements, thus not allowing its detection. The stability constants obtained from UV/Vis measurements were 13.23 ± 0.03 , 5.58 ± 0.02 and 26.71 ± 0.01 , for $[\text{Ga}(\text{8-HQA})]^+$, $[\text{Ga}(\text{8-HQA})(\text{OH})_2]^-$ and $[\text{Ga}(\text{8-HQA})_2]^-$, respectively. As observed, these values are slightly higher than those obtained by potentiometry, especially for the last two species. This can be ascribed to the wider pH range investigated during spectrophotometric measurements (with respect to potentiometric experiments), in which the $\text{Ga}(\text{OH})_4^-$ species becomes dominant. In this case, the above-cited overestimated value of its hydrolysis constant determines its higher formation, thus affecting all refined values of the stability constants of species formed in that pH range. In fact, just lowering the input value of this hydrolysis constant from $\log \beta = -16.78$ (that is used in the model and comes from literature data analysis as described above) to $\log \beta = -18$ gives a refined value of $\log \beta \sim 4.9 \pm 0.1$ for the $[\text{Ga}(\text{8-HQA})(\text{OH})_2]^-$ species, which is perfectly in line with potentiometric findings. In fact, during potentiometric measurements, in which most of titrations were stopped at $\text{pH} \sim 7.5$, the formation of the $[\text{Ga}(\text{OH})_4]^-$ species is lower, thus leading to a less marked effect during data analysis and more reliable values of the refined constants. Spectrophotometric data analysis also allowed the calculation of the specific molar absorbances of the observed species, plotted in Fig. 2 in the $200 \leq \lambda / \text{nm} \leq 500$ wavelength range.

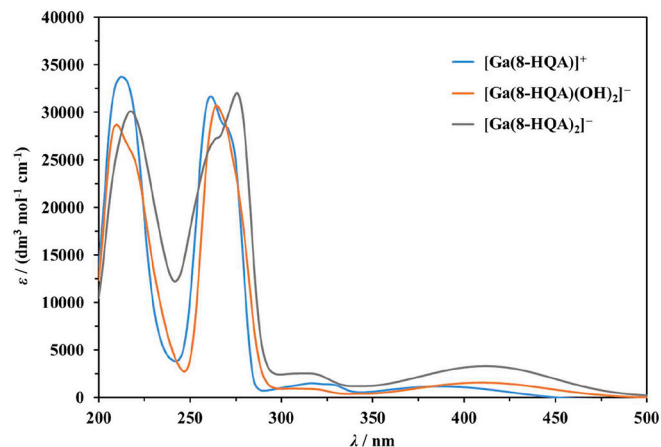


Fig. 2. Specific molar absorbances of $\text{Ga}_p(\text{8-HQA})_q\text{H}_r$ species at different wavelengths, at.

$I = 0.2 \text{ mol dm}^{-3}$ in $\text{KCl}_{(\text{aq})}$ and $T = 298.15 \text{ K}$.

3.1.3. UV/Vis spectrophotometric competition measurements between Ga^{3+} and Fe^{3+}

In order to check the reliability of stability constants determined, especially in relation to the main $[\text{Ga}(\text{8-HQA})_2]^-$ species and in comparison with analogous $\text{Fe}_p(\text{8-HQA})_q\text{H}_r$ species, we also performed some metal competition UV/Vis measurements (details given in Table S2), by titrating $\text{Ga}^{3+}/\text{8-HQA}$ solutions at $\text{pH} \sim 3.5\text{--}4.0$ with Fe^{3+} , and vice versa. Two examples of curves are shown in Fig. 3. In these conditions, only $[\text{M}(\text{8-HQA})]^+$ and $[\text{M}(\text{8-HQA})_2]^-$, with $\text{M} = \text{Ga}$ or Fe , can be formed according to the speciation models obtained for both cations. The data analysis by HypSpec software required the preliminary determination of the specific molar absorbances of $[\text{Fe}(\text{8-HQA})]^+$ and $[\text{Fe}(\text{8-HQA})_2]^-$ species to be used as input. Dedicated measurements were thus performed, resulting in refined stability constants in agreement with already published data (*i.e.*, $\log \beta = 13.91 \pm 0.01$ and 26.26 ± 0.02 for $[\text{Fe}(\text{8-HQA})]^+$ and $[\text{Fe}(\text{8-HQA})_2]^-$, respectively, vs. $\log \beta = 13.9$ and 26.95 of ref. [7]) and the specific molar absorbance spectra, shown in Fig. S2. Afterwards, data analysis of metal competition experiments gave, as result, $\log \beta = 26.23 \pm 0.01$ for the main $[\text{Ga}(\text{8-HQA})_2]^-$ species, which is in very good agreement with the analogous value obtained by potentiometry. A speciation diagram of 8-HQA in the presence of both Ga^{3+} and Fe^{3+} is presented in Fig. S3.

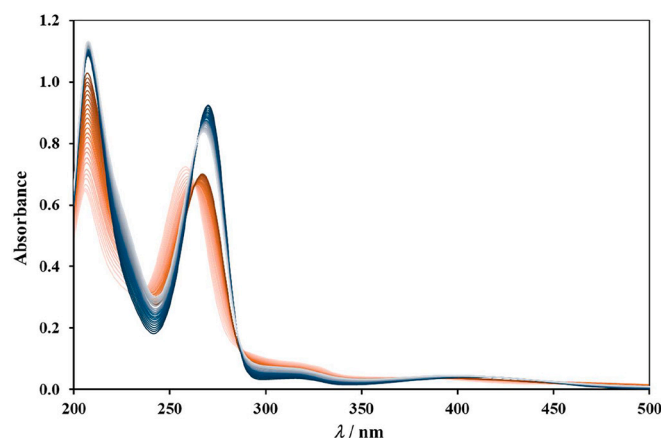


Fig. 3. UV/Vis spectrophotometric titrations of $\text{Ga}^{3+}/\text{8-HQA}$ solutions at $\text{pH} \sim 3.5\text{--}4.0$ with Fe^{3+} (blue) and vice versa (orange). Blue spectra: $c_{\text{8-HQA}} = 2 \times c_{\text{Ga}} = 3.0 \times 10^{-5} \text{ mol dm}^{-3}$, $c_{\text{Fe}} = 4.0 \times 10^{-4} \text{ mol dm}^{-3}$ as titrant. Orange spectra: $c_{\text{8-HQA}} = 2 \times c_{\text{Fe}} = 3.0 \times 10^{-5} \text{ mol dm}^{-3}$, $c_{\text{Ga}} = 4.0 \times 10^{-4} \text{ mol dm}^{-3}$ as titrant. (For interpretation of the references to colour in this figure legend, the reader is referred to the web version of this article.)

3.1.4. Formation and stability of $\text{Ga}^{3+}/\text{EDTA}$ species

As previously stated, the expected high stability of the $\text{Ga}^{3+}/8\text{-HQA}$ complexes imposed additional application of the ligand-competition approach. According to this method, potentiometric titrations were also performed for the investigated system in the presence of EDTA as competing ligand in the complexation equilibria. There are two important conditions for such approach to be applied. First, the stability constants of the complexes between the competing ligand and the metal cation under study must be comparable to those of the ligand of interest. In this way, the competition between the two ligands hampers the complete proton displacement from the investigated ligand, causing its potentiometric titration by ISE-H^+ to be reliable. Second, it is crucial that the stability constants of the competing ligand are known in the exact conditions of the system under investigation, and are as accurate as possible, since the values of refined constants depends on those values.

In the case of $\text{Ga}^{3+}/8\text{-HQA}$ complexes, it is worth mentioning that this approach would not strictly be needed, since even water acts as a competing ligand, due to the strong hydrolysis of Ga^{3+} cation that already occurs at low pH values. Furthermore, it was essential to know the stability constants of $\text{Ga}^{3+}/\text{EDTA}$ complexes under the experimental conditions applied (i.e., $I = 0.2 \text{ mol dm}^{-3}$ in $\text{KCl}_{(\text{aq})}$ and $T = 298.15 \text{ K}$). Despite a thorough literature search, it was not possible to find any data for these particular conditions [40], though they are often used for studies of biologically relevant systems. As such, it has been decided in this work to follow the same approach previously adopted for the study of the $\text{Fe}^{2+}/8\text{-HQA}$ and $\text{Fe}^{3+}/8\text{-HQA}$ systems [7], i.e., to design a set of experiments in which the simultaneous determination of both $\text{Ga}_p(\text{EDTA})_q\text{H}_r$ and $\text{Ga}_p(8\text{-HQA})_q\text{H}_r$ species was possible, thanks to a high number of experiments planned in a wide range of 8-HQA, EDTA and Ga^{3+} concentrations and ratios (Table S1). In fact, as it is true that EDTA competes with 8-HQA towards Ga^{3+} complexation, the same holds for 8-HQA with EDTA.

The stability constants of the $[\text{Ga}(\text{EDTA})]^-$ and $[\text{Ga}(\text{EDTA})(\text{OH})]^{2-}$ species, determined for the first time at $I = 0.2 \text{ mol dm}^{-3}$ in $\text{KCl}_{(\text{aq})}$ and $T = 298.15 \text{ K}$ and reported in Table 2, resulted in good agreement with literature values, if the different conditions are taken into account. To better visualize competition between the two ligands, a speciation diagram of the $\text{Ga}^{3+}/8\text{-HQA}/\text{EDTA}$ system is presented in Fig. S4.

3.1.5. ESI-MS analysis of $\text{Ga}^{3+}/8\text{-HQA}$ system in aqueous solution

The analysis of the stability constants of $\text{Ga}^{3+}/8\text{-HQA}$ complexes reported in Table 2, and the speciation diagram in Fig. 1, clearly indicate that $[\text{Ga}(8\text{-HQA})_2]^-$ is the predominant species. ESI-MS measurements were performed on several samples, using different $c_{\text{L}}:c_{\text{M}}$ ratios, and in both positive and negative polarity modes. Mass spectra obtained in the negative mode (Fig. 4) show the formation of a peak at $m/z = 443.05$, with the isotopic pattern consistent with the presence of this species ($[\text{Ga}(8\text{-HQA})_2]^-$, $\text{C}_{20}\text{H}_{10}\text{GaN}_2\text{O}_6^-$, $m/z = 442.98$).

3.2. Solid state studies: Synthesis and physicochemical characterization of $\text{Ga}^{3+}/8\text{-HQA}$ complexes

For comparative purposes, and for a better insight on the coordination mode of 8-HQA towards Ga^{3+} ions, the synthesis of the $\text{Ga}^{3+}/8\text{-HQA}$ complexes was performed. A complete physicochemical characterization of the synthesized metal complexes has been performed to confirm metal complex formation in solid state and to identify the formed species. The change in colour of the solutions after addition of metal suspension was the first indication of the coordination process. From the different experimental conditions tested (see dedicated section), the formation of an amorphous precipitate was observed, only after (slow) evaporation of the reaction solvent. After isolation, washing and drying, the obtained precipitates were analyzed. The colors of obtained precipitates were different, depending on the addition (orange/light brown) or the absence (dark brown) of Et_3N in the reaction

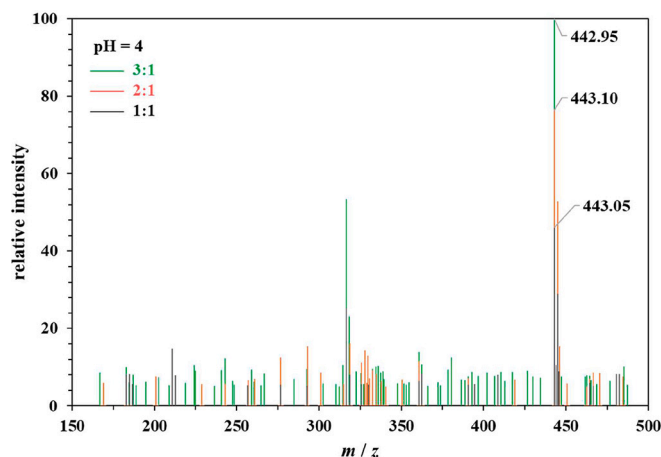


Fig. 4. Superimposed ESI-MS spectra of $\text{Ga}^{3+}/8\text{-HQA}$ solutions at different $c_{8\text{-HQA}}:c_{\text{Ga}}$ ratios, at pH = 4. Black lines: $c_{8\text{-HQA}}:c_{\text{Ga}} = 1:1$; red lines: $c_{8\text{-HQA}}:c_{\text{Ga}} = 2:1$; green lines: $c_{8\text{-HQA}}:c_{\text{Ga}} = 3:1$. (For interpretation of the references to colour in this figure legend, the reader is referred to the web version of this article.)

mixture. No formation of crystals was observed.

3.2.1. ATR-FTIR analysis

All obtained precipitates were first analyzed by ATR-FTIR. The main differences between the ATR-FTIR spectra of 8-HQA and those of the isolated precipitates are observed in the region of the O—H vibrations (see Fig. S5). The attribution of the bands was based on information given in refs. [46–48]. In particular, the bands registered for the free ligand at 3267 cm^{-1} and 3043 cm^{-1} , characteristic of the O—H stretching of the phenol group and the carboxylic acid, respectively, in the case of the isolated precipitate are changed into a large and not defined band, centered at around 2900 cm^{-1} . Even the characteristic band of the quinolinic N (3147 cm^{-1}) is part of the mentioned broad band. Worth of mention is also the shift observed in the C=O stretching band (from 1807 cm^{-1} to 1725 cm^{-1}). This is a clear evidence of the formation of the $\text{Ga}^{3+}/8\text{-HQA}$ metal complex, with the carboxylic, the phenol and the heterocyclic N involved.

3.2.2. ESI-MS analysis

After confirmation that the isolated precipitates correspond to the Ga^{3+} complexes, the samples were investigated by ESI-MS. Fig. S6 shows an example of the obtained ESI-MS spectra. In all the ESI- spectra we could observe the presence of a peak at $m/z \sim 443$, corresponding to the $[\text{Ga}(8\text{-HQA})_2]^-$ species ($\text{C}_{20}\text{H}_{10}\text{GaN}_2\text{O}_6^-$, $m/z = 442.98$). On ESI+ spectra, the observed peak at $m/z \sim 489$ corresponds to the Na^+ adduct ($[\text{Ga}(8\text{-HQA})_2(\text{Na})_2]^+$, $\text{C}_{20}\text{H}_{10}\text{GaN}_2\text{Na}_2\text{O}_6^+$, $m/z = 488.96$). Other adducts were also identified, as indicated in Table 3.

Table 3

Proposed formulas of species identified by ESI-MS in the isolated precipitate of the synthesis at $c_{8\text{-HQA}}:c_{\text{Ga}} = 2:1$ ratio, without the addition of Et_3N , based on the calculated and experimental m/z values.

	Adduct Formula	Molecular formula	exp. m/z	calc. m/z
ESI-	$[\text{Ga}(8\text{-HQA})_2]^-$	$(\text{C}_{20}\text{H}_{10}\text{GaN}_2\text{O}_6^-)$	442.89	442.98
	$[\text{Ga}(8\text{-HQA})(\text{HCOO})_2(\text{H}_2\text{O})_3]^-$	$(\text{C}_{12}\text{H}_{13}\text{GaNO}_{10})$	399.97	399.98
	$[\text{Ga}(8\text{-HQA})_2(\text{Na})_2]^+$	$(\text{C}_{20}\text{H}_{10}\text{GaN}_2\text{Na}_2\text{O}_6^+)$	488.91	488.96
ESI+	$[\text{Ga}(8\text{-HQA})(\text{HCOOH})(\text{H}_2\text{O})]^+$	$(\text{C}_{11}\text{H}_9\text{GaNO}_6^+)$	319.80	319.97
	$[(8\text{-HQA})(\text{H}_2)(\text{H}_2\text{O})_2(\text{H})]^+$	$(\text{C}_{10}\text{H}_{12}\text{NO}_5^+)$	225.92	226.07

3.2.3. TGA

The same precipitates were also analyzed by thermogravimetric analysis (see Fig. S7). The residual mass was 17.75%, and the only stable species up to 1273.15 K is Ga₂O₃ oxide. The calculation of the experimental molar mass determined from the residual solid was based on the following equation:

$$M_{\text{exp}} = \frac{M_{\text{residual solid}} \times \text{stoichiometric factor of the metal content} \times 100\%}{\text{residual mass\%}} \quad (5)$$

Different species were hypothesized, considering the presence of solvent molecules in the isolated solid, evidenced by the loss of mass observed at low temperature range. With that in mind, [Ga(8-HQA)₂(H₂O)₂].MeOH.0.5H₂O presented the lowest difference (~1.1%) between the experimental and the calculated molar mass (i.e., 528.01 g mol⁻¹ vs. 522.1 g mol⁻¹, respectively), which is in agreement with estimated accuracy of the technique (1–2%). The high temperature needed for the release of the H₂O molecules led us to consider that they are partially coordinated to the metal center.

3.3. Effect of 8-HQA and its Ga³⁺ complexes on microbiota radiosensitivity

Considering the presence of 8-HQA as a tryptophan metabolite in the human gut and to get a better insight into their action in the microbiota, we studied the possible protection effect of 8-HQA and its Ga³⁺ complex on different bacteria submitted to ionizing γ -radiation. The bacterial isolates used in this study included *Actinomyces viscosus*, *Streptococcus mutans*, *Streptococcus sobrinus*, isolated from human oral cavity, and *Pseudomonas putida*, *Pseudomonas fluorescens* and *Escherichia coli*, characteristic of the gut microbiota.

The study started by the assessment of the susceptibility of each microbe to the compounds of interest and it was accomplished by the disk diffusion test method [35], as described in the dedicated experimental section. There was no evidence of antibacterial activity by the compounds against the analyzed bacteria, at the tested concentrations, with the exception of Ga(NO₃)₃ over *Streptococcus spp.*, which presented, nevertheless, a very small susceptibility effect ($\phi < 1.0$ cm). These results allowed us to proceed with the irradiation experiments, as the observed results would only be a direct consequence of the radiation exposure.

When ionizing radiation is absorbed by biological material, it interacts with critical cellular targets. Large biomolecules like DNA, RNA, and proteins may be ionized or excited through direct energy deposition, initiating a chain of events that can lead to cell inactivation, a process known as the direct effect of radiation. Another major target of ionizing radiation in the cell is water, the most abundant molecule. This interaction leads to the formation of highly reactive free radicals as a result of water radiolysis. The radicals formed, including solvated electrons (e_s⁻), hydrogen atoms (H[•]), hydroxyl radicals (OH[•]), hydrogen molecules (H₂), and hydrogen peroxide (H₂O₂), react with DNA and other critical biological targets, which can also result in cell inactivation. This process is known as the indirect effect of radiation. The sensitivity of microorganisms to radiation depends on both biotic (intrinsic) and abiotic (extrinsic) factors. Biotic factors include differences between species and strains of the organisms, cell wall compositions, growth phase, and intrinsic mechanisms to recover from radiation injuries (e.g., enzymatic repair of DNA breaks). Abiotic factors comprise external influences such as from temperature, atmosphere and substrate. Part of the effect of ionizing radiation on microorganisms is due to indirect action mediated through radicals. The medium (substrate) in which microorganisms are suspended plays a crucial role in determining the dose required for a given microbicidal effect. In more complex media, competition from media components for the free radicals formed by irradiation within the cell increases, thereby “sparing” or “protecting” the microorganisms. Some chemical components of the substrate medium can increase radioresistance (protective effect), while others can lower it (sensitizing

effect). The presence of scavengers that react with free radicals liberated from water radiolysis will protect or reduce the radiation damage to cells normally attacked by these radicals. Further details can be found in ref. [49].

The samples containing the bacterial suspension (3–4 × 10⁶ cell cm⁻³) and the compound of interest (~1 mg cm⁻³) were divided in four groups: non-irradiated (0 kGy), 0.175 kGy, 0.35 kGy, and 0.525 kGy irradiated samples. The D₁₀ values (i.e., the dose required for 90% inactivation of the initial population) were determined according to the surviving curves presented in Fig. 5 for *A. viscosus* and Figs. S8–S12 for other tested bacteria. In practical terms, the loss of colony-forming ability by cells when they are grown on nutrient medium is commonly assumed as a criterion of radiation-induced damage; cells that have lost this competence are reported to be inactivated or non-viable by the action of ionizing radiation.

In fact, surprisingly, the substrate of Ga³⁺/8-HQA complex suggested to have an antibacterial effect against tested *Streptococcus* strains, as no viable colony of *S. mutans* was detected and only a few *S. sobrinus* colonies were observed in the non-irradiated sample, while all the irradiated samples did not present growth viability (Figs. S11 and S12). These results are contrary to those obtained with the disk diffusion method. A possible explanation could be the fact that the conditions used in both procedures are different (suspension vs. soaked disk), which may induce a different effect of the metal complex towards the bacteria. Furthermore, for *Streptococcus* isolates, a possible radiosensitizing effect of metal could be considered. It is worth of mention that, for *E. coli* and *P. putida*, a deviation from the linear correlation was observed for higher doses of radiation, as the result of the high sensitivity of these strains to radiation. Therefore, the experiment was redesigned using a lower absorbed doses (0.07 and 0.14 kGy) for the determination of D₁₀ values.

The calculated D₁₀ values obtained for each bacterium, presented in Table 4, indicate that, among the analyzed isolates, the most radiosensitive is *E. coli* (lower D₁₀ values). The D₁₀ values of *Pseudomonas* and *E. coli* strains indicated no statistical difference ($P > 0.05$) among the physiological serum, 8-HQA and Ga³⁺/8-HQA substrates, suggesting that the ligand and its Ga³⁺ complex have no effect on their radiosensitivity. This lack of substrate effect was also observed for *S. sobrinus* when comparing physiologic serum and ligand compounds. Although, for *A. viscosus* and *S. mutans*, a significant ($P < 0.05$) increase of D₁₀ value was observed when suspended in Ga³⁺/8-HQA complex and 8-HQA solutions, respectively, expressing a radioprotective effect of these substrates. This could highlight a scavenging effect of the complex on the highly reactive species formed by water radiolysis, preventing their capacity to cause damage on microbial cells.

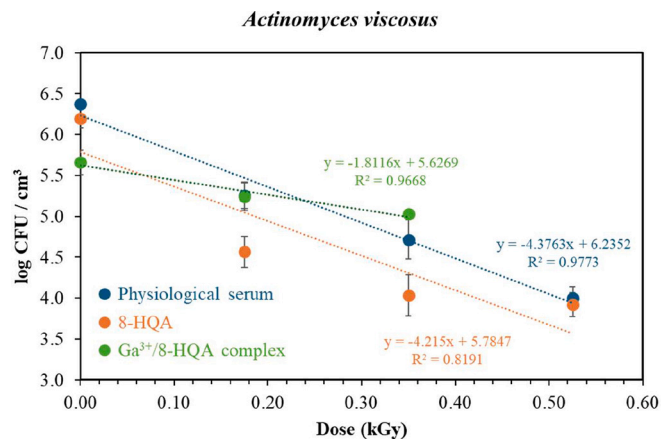


Fig. 5. Survival curves for *Actinomyces viscosus* in physiological serum suspensions and in the presence of 8-HQA and Ga³⁺/8-HQA complex. Error bars represent 95% confidence interval.

Table 4

Average D_{10} values (required dose for 90% inactivation of the initial population) calculated for each bacterium^a

	Physiological serum	8-HQA	Ga ³⁺ /8-HQA complex	Ga (NO ₃) ₃
<i>Actinomyces viscosus</i>	0.229 ± 0.05 *	0.24 ± 0.01 *	0.551 ± 0.006	n.d.
<i>Streptococcus mutans</i>	0.100 ± 0.002 *	0.134 ± 0.006	n.s.	n.d.
<i>Streptococcus sobrinus</i>	0.11 ± 0.01	0.128 ± 0.003	n.s.	n.d.
<i>Escherichia coli</i>	0.0608 ± 0.0009	0.072 ± 0.003	0.068 ± 0.005	n.s.
<i>Pseudomonas putida</i>	0.09 ± 0.01	0.12 ± 0.03	0.15 ± 0.01	n.s.
<i>Pseudomonas fluorescens</i>	0.136 ± 0.003	0.11 ± 0.03	0.119 ± 0.008	n.s.

^a ± standard deviation; n.d.: not determined; n.s.: no cellular survival. Values with asterisks (*) are significantly different ($P < 0.05$) from others.

3.4. Anti-proliferative and anti-inflammatory assays

Taking into account that, as above-stated, the kynurenine pathway is related to the immune system through the inflammatory response [4], we also evaluated the anti-inflammatory activity of 8-HQA and its Ga³⁺ complex. For that purpose, the Griess assay was used, following the procedure described in the experimental section. The Griess reaction is a straightforward spectrophotometric method (at $\lambda = 540$ nm) for analyzing nitrites (NO₂⁻) in aqueous solutions. The implemented methodology must begin by confirming that the compounds under investigation have no anti-proliferative effect on the cell line used (RAW 264.7 murine macrophage cells), utilizing the WST-1 assay. In fact, no anti-proliferative activity on RAW 264.7 cells was observed for any of the tested compounds (Fig. S13), at the tested concentrations (cell viability ca. 100%), pointing out the absence of compounds' cytotoxicity. With this result, it was possible to proceed for the anti-inflammatory assays, knowing that 8-HQA and its Ga³⁺ complex will not affect the cells growth.

The inflammatory process is recognized as protective reaction towards trauma, infection, tissue injury or noxious stimuli. During this process, activated inflammatory cells (e.g., neutrophils, eosinophils, mononuclear phagocytes, and macrophages) release elevated levels of nitric oxide (NO), prostaglandin E2 (PGE2), and cytokines, including interleukin (IL)-1 β , IL-6, and tumor necrosis factor (TNF). These substances not only cause cell and tissue damage, but also activate macrophages in diseases like rheumatoid arthritis and chronic hepatitis. LPS stimulation alone has been shown to induce Nitric Oxide Synthases (NOS), transcription and protein synthesis in murine macrophage RAW 264.7 cells, leading to a corresponding increase in NO production [39]. Considering all this, the anti-inflammatory results are shown in Fig. 6, where it can be observed that 8-HQA has actually an increasing effect on the production of NO₂⁻, statistically significant ($P < 0.05$) for the concentrations of 2 and 4 mmol dm⁻³ compared to control, which could indicate of a higher inflammation ability. On the contrary, Ga³⁺/8-HQA complex seems to lead to a significant decrease ($P < 0.05$) of ca. 30% on NO₂⁻ production for the concentration of 0.5 mmol dm⁻³. These results indicate that Ga³⁺/8-HQA complex may suppress NO generation activity, without inducing cytotoxicity, probably by inhibiting the NOS, showing anti-inflammatory potential.

4. Conclusions

The chemical speciation of Ga³⁺ in the presence of 8-hydroxyquinoline-2-carboxylic acid (8-HQA) has been investigated. Among all the formed species, [Ga(8-HQA)₂]⁻ is the most stable in a wide pH range, as also confirmed by ESI-MS analysis. The chemical speciation of the Ga³⁺/8-HQA system is similar to the analogue Fe³⁺/8-HQA, in terms of both

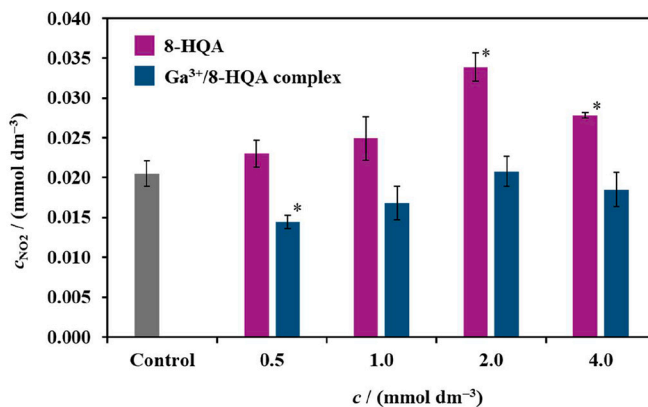


Fig. 6. Anti-inflammatory assay using RAW264.7 cells in the presence of 8-HQA and Ga³⁺/8-HQA complex. Error bars represent 95% confidence interval. * Significantly different ($P < 0.05$) from control.

nature and stability of formed complexes. However, this is not reflected in the sequestering ability of 8-HQA towards both cations. In fact, calculated $pL_{0.5}$ (an empirical parameter used, for comparison purposes, to quantify the sequestering ability of a ligand towards a given cation in particular conditions) are 4.79 and 8.42 at pH = 7.4 (and in the experimental conditions of this work), for Ga³⁺ and Fe³⁺ (from ref. [7]), respectively, indicating a great preference of 8-HQA towards Fe³⁺ (the higher the $pL_{0.5}$, the higher the sequestering ability). Further details about the meaning, calculation and use of $pL_{0.5}$ are given in refs. [50, 51]. This is due to the slightly different hydrolytic behavior of both cations, since the formation of Ga³⁺ hydroxo species compete with 8-HQA in a higher extent than those of Fe³⁺. This is also reflected in a significant decrease of the sequestering ability of 8-HQA towards Ga³⁺ with increasing pH, as depicted in Fig. 7 ($pL_{0.5}$ vs. pH). This behavior is a strong confirmation of the relevance of the use of a correct data set of hydrolysis constants. For this reason, a critical literature analysis of Ga³⁺ hydrolysis constants has been performed in this work, providing equations for their calculation in a wide range of experimental conditions. Noteworthy, thanks to a proper experimental design, the stability constants of [Ga(EDTA)]⁻ and [Ga(EDTA)(OH)]²⁻ were also determined, for the first time in the conditions of this work. The solid-state studies here presented also show that [Ga(8-HQA)₂]⁻ is the main complex species formed. Regarding the effects of this species in human microbiota response to ionizing radiation, it can be highlighted a radioprotective effect in *Actinomyces viscosus*, and a potential radiosensitizing effect against *Streptococcus mutans* and *Streptococcus sobrinus*. When exploring additional biological properties, the obtained results suggested no cytotoxicity of tested compounds on RAW264.7 murine macrophage cells stressing an anti-inflammatory potential of Ga³⁺/8-

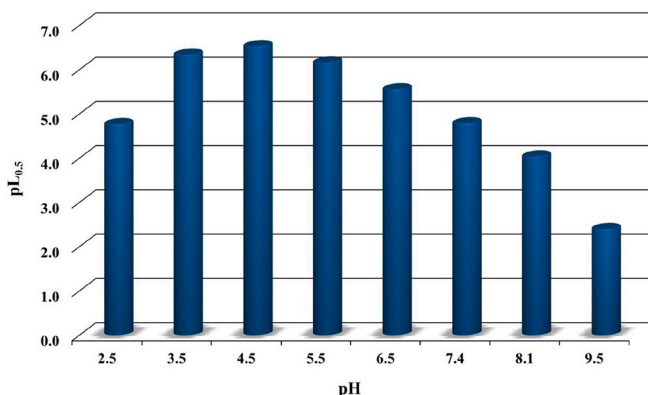


Fig. 7. Sequestering ability ($pL_{0.5}$) of 8-HQA towards Ga³⁺, as a function of pH.

HQA complex.

CRedit authorship contribution statement

Izabela Ryza: Writing – original draft, Visualization, Investigation. **Claudia Granata:** Writing – original draft, Visualization, Investigation. **Nadia Ribeiro:** Writing – original draft, Investigation. **Edyta Nalewajko-Sieliwoniuk:** Writing – original draft, Investigation. **Andreas Kießling:** Visualization, Investigation. **Marta Hryniewicka:** Visualization, Investigation. **Winfried Plass:** Writing – review & editing, Validation, Supervision, Resources, Methodology, Formal analysis. **Beata Godlewska-Żyłkiewicz:** Writing – review & editing, Validation, Supervision, Resources, Methodology, Formal analysis. **Sandra Cabo Verde:** Writing – review & editing, Validation, Supervision, Resources, Methodology, Formal analysis. **Demetrio Milea:** Writing – review & editing, Visualization, Validation, Supervision, Resources, Project administration, Methodology, Funding acquisition, Formal analysis, Data curation, Conceptualization. **Sofia Gama:** Writing – review & editing, Visualization, Validation, Supervision, Resources, Project administration, Methodology, Funding acquisition, Formal analysis, Data curation, Conceptualization.

Declaration of competing interest

The authors declare the following financial interests/personal relationships which may be considered as potential competing interests: Sofia Gama reports financial support was provided by National Science Centre Poland. Demetrio Milea reports financial support was provided by Italian Ministry of University and Research. Sandra Cabo Verde reports financial support was provided by Foundation for Science and Technology. If there are other authors, they declare that they have no known competing financial interests or personal relationships that could have appeared to influence the work reported in this paper.

Data availability

Data will be made available on request.

Acknowledgements

The authors would like to thank the financial support from the National Science Centre (NCN), Poland, under the scope of the research project number 2020/39/B/ST4/03060. Authors would also like to acknowledge the MS platform at the Friedrich Schiller University Jena for support in mass spectrometry. DM acknowledges financial support under the National Recovery and Resilience Plan (NRRP), Mission 4, Component 2, Investment 1.1, Call for tender No. 1409 published on 14.9.2022 by the Italian Ministry of University and Research (MUR), funded by the European Union – NextGenerationEU – Project Title Efficient Sequestration of Metal Ions from Aqueous Systems for Green and Sustainable Applications - AquaGreen – CUP J53D23014430001 – Grant Assignment Decree No. 1409 adopted on 14/09/2022 by the Italian Ministry of Ministry of University and Research (MUR). C²TN authors are grateful to the Foundation for Science and Technology (FCT, Portugal) for the financial support through UID/Multi/04349/2020.

Appendix A. Supplementary data

Supplementary data to this article can be found online at <https://doi.org/10.1016/j.jinorgbio.2024.112670>.

References

- [1] E. Ahmed, S.J. Holmstrom, Siderophores in environmental research: roles and applications, *Microb. Biotechnol.* 7 (2014) 196–208, <https://doi.org/10.1111/1751-7915.12117>.

- [2] K. Walczak, E. Langner, K. Szalast, A. Makuch-Kocka, P. Pozarowski, T. Plech, *Molecules* 25 (2020).
- [3] J. Pesek, J. Svoboda, M. Sattler, S. Bartram, W. Boland, Biosynthesis of 8-hydroxyquinoline-2-carboxylic acid, an iron chelator from the gut of the lepidopteran *Spodoptera littoralis*, *Org. Biomol. Chem.* 13 (2015) 178–184, <https://doi.org/10.1039/c4ob01857e>.
- [4] M. Ala, The footprint of kynurenine pathway in every cancer: a new target for chemotherapy, *Eur. J. Pharmacol.* 896 (2021) 173921, <https://doi.org/10.1016/j.ejphar.2021.173921>.
- [5] J.C. Deschemin, M.L. Noordine, A. Remot, A. Willemetz, C. Afif, F. Canonne-Hergaux, P. Langella, Z. Karim, S. Vaulont, M. Thomas, G. Nicolas, The microbiota shifts the iron sensing of intestinal cells, *FASEB J.* 30 (2016) 252–261, <https://doi.org/10.1096/fj.15-276840>.
- [6] M. Funke, R. Buchler, V. Mahobia, A. Schneeberg, M. Ramm, W. Boland, Rapid hydrolysis of quorum-sensing molecules in the gut of lepidopteran larvae, *Chembiochem* 9 (2008) 1953–1959, <https://doi.org/10.1002/cbic.200700781>.
- [7] S. Gama, M. Frontauria, N. Ueberschaar, G. Brancato, D. Milea, S. Sammartano, W. Plass, Thermodynamic study on 8-hydroxyquinoline-2-carboxylic acid as a chelating agent for iron found in the gut of noctuid larvae, *New J. Chem.* 42 (2018) 8062–8073, <https://doi.org/10.1039/c7nj04889k>.
- [8] T. Emery, P.B. Hoffer, Siderophore-mediated mechanism of gallium uptake demonstrated in the microorganism *Ustilago sphaerogena*, *J. Nucl. Med.* 21 (1980) 935–939.
- [9] Y. Kaneko, M. Thoendel, O. Olakanmi, B.E. Britigan, P.K. Singh, The transition metal gallium disrupts *Pseudomonas aeruginosa* iron metabolism and has antimicrobial and antibiofilm activity, *J. Clin. Invest.* 117 (2007) 877–888, <https://doi.org/10.1172/JCI30783>.
- [10] J.A. Lemire, J.J. Harrison, R.J. Turner, Antimicrobial activity of metals: mechanisms, molecular targets and applications, *Nat. Rev. Microbiol.* 11 (2013) 371–384, <https://doi.org/10.1038/nrmicro3028>.
- [11] M.A. Green, M.J. Welch, Gallium radiopharmaceutical chemistry, *Int. J. Rad. Appl. Instrum. B* 16 (1989) 435–448, [https://doi.org/10.1016/0883-2897\(89\)90053-6](https://doi.org/10.1016/0883-2897(89)90053-6).
- [12] J. Clausen, C.J. Edeling, J. Fogh, 67Ga binding to human serum proteins and tumor components, *Cancer Res.* 34 (1974) 1931–1937.
- [13] S.W. Gunasekera, L.J. King, P.J. Lavender, The behaviour of tracer gallium-67 towards serum proteins, *Clin. Chim. Acta* 39 (1972) 401–406, [https://doi.org/10.1016/0009-8981\(72\)90059-9](https://doi.org/10.1016/0009-8981(72)90059-9).
- [14] A. Braud, M. Hannauer, G.L. Mislin, L.J. Schalk, The *Pseudomonas aeruginosa* pyochelin-iron uptake pathway and its metal specificity, *J. Bacteriol.* 191 (2009) 3517–3525, <https://doi.org/10.1128/JB.00010-09>.
- [15] M. Fani, H.R. Maecke, S.M. Okarvi, Radiolabeled peptides: valuable tools for the detection and treatment of cancer, *Theranostics* 2 (2012) 481–501, <https://doi.org/10.7150/thno.4024>.
- [16] D. Front, R. Bar-Shalom, R. Epelbaum, N. Haim, M.W. Ben-Arush, M. Ben-Shahar, M. Gorenberg, U. Kleinhaus, S. Parmett, G.M. Kolodny, et al., Early detection of lymphoma recurrence with gallium-67 scintigraphy, *J. Nucl. Med.* 34 (1993) 2101–2104.
- [17] C.J. Palestro, The current role of gallium imaging in infection, *Semin. Nucl. Med.* 24 (1994) 128–141, [https://doi.org/10.1016/s0001-2998\(05\)80227-2](https://doi.org/10.1016/s0001-2998(05)80227-2).
- [18] M.U. Khan, S. Khan, S. El-Refaie, Z. Win, D. Rubello, A. Al-Nahhas, Clinical indications for Gallium-68 positron emission tomography imaging, *Eur. J. Surg. Oncol.* 35 (2009) 561–567, <https://doi.org/10.1016/j.ejso.2009.01.007>.
- [19] G. Lapinska, M. Bryszewska, A. Fijolek-Warszewska, I. Kozłowicz-Gudzinska, P. Ochman, A. Sackiewicz-Slaby, The diagnostic role of 68Ga-DOTATATE PET/CT in the detection of neuroendocrine tumours, *Nucl. Med. Rev. Cent. East. Eur.* 14 (2011) 16–20, <https://doi.org/10.5603/nmr.2011.0004>.
- [20] N.P. Lenzo, D. Meyrick, J.H. Turner, Review of Gallium-68 PSMA PET/CT imaging in the Management of Prostate Cancer, *Diagnostics (Basel)* 8 (2018) 16, <https://doi.org/10.3390/diagnostics8010016>.
- [21] S.R. Banerjee, M.G. Pomper, Clinical applications of Gallium-68, *Appl. Radiat. Isot.* 76 (2013) 2–13, <https://doi.org/10.1016/j.apradiso.2013.01.039>.
- [22] A. Yokoyama, Y. Ohmomo, K. Horiuchi, H. Saji, H. Tanaka, K. Yamamoto, Y. Ishii, K. Torizuka, Deferoxamine, a promising bifunctional chelating agent for labeling proteins with gallium: Ga-67 DF-HSA: concise communication, *J. Nucl. Med.* 23 (1982) 909–914.
- [23] A. Barylka, B. Godlewska-Żyłkiewicz, D. Milea, S. Gama, The accurate assessment of the chemical speciation of complex systems through multi-technique approaches, *Pure Appl. Chem.* (2024), <https://doi.org/10.1515/pac-2024-0206>.
- [24] W.R. Harris, A.E. Martell, Aqueous complexes of gallium(III), *Inorg. Chem.* 15 (2002) 713–720, <https://doi.org/10.1021/ic50157a044>.
- [25] R. Delgado, M. do Carmo Figueira, S. Quintino, Redox method for the determination of stability constants of some trivalent metal complexes, *Talanta* 45 (1997) 451–462, [https://doi.org/10.1016/s0039-9140\(97\)00157-4](https://doi.org/10.1016/s0039-9140(97)00157-4).
- [26] A.E. Martell, R.J. Motekaitis, *Determination and Use of Stability Constants*, VCH Publishers, New York, 1992.
- [27] C. Bretti, R.M. Cigala, G. Lando, D. Milea, S. Sammartano, Sequestering ability of phytate toward biologically and environmentally relevant trivalent metal cations, *J. Agric. Food Chem.* 60 (2012) 8075–8082, <https://doi.org/10.1021/jf302007v>.
- [28] R. Huang, J. Xiang, P. Zhou, Vitamin D, gut microbiota, and radiation-related resistance: a love-hate triangle, *J. Exp. Clin. Cancer Res.* 38 (2019) 493, <https://doi.org/10.1186/s13046-019-1499-y>.
- [29] H.A. Flaschka, *EDTA Titrations, An Introduction to Theory and Practice*, Pergamon, Amsterdam, 1964.
- [30] T. Dudev, C. Lim, Competition among metal ions for protein binding sites: determinants of metal ion selectivity in proteins, *Chem. Rev.* 114 (2014) 538–556, <https://doi.org/10.1021/cr4004665>.

- [31] A. Baryłka, A. Bagińska-Krakówka, L. Zuccarello, F. Mancuso, G. Gattuso, G. Lando, C. Sgarlata, C. De Stefano, B. Godlewska-Żyłkiewicz, D. Milea, S. Gama, Protonation equilibria of the tryptophan metabolite 8-hydroxyquinoline-2-carboxylic acid (8-HQA) and its precursors: a potentiometric and calorimetric comparative study, *Thermochim. Acta* 730 (2023) 179615, <https://doi.org/10.1016/j.tca.2023.179615>.
- [32] C. De Stefano, P. Mineo, C. Rigano, S. Sammartano, Ionic strength dependence of formation constants, in: XVII. The Calculation of Equilibrium Concentrations and Formation Constants, *Ann. Chim. (Rome)* vol. 83, 1993, pp. 243–277.
- [33] P. Gans, Hyperquad. <http://www.hyperquad.co.uk/>, 2024 (accessed May 2024).
- [34] L. Castellino, E. Alladio, S. Bertinetti, G. Lando, C. De Stefano, S. Blasco, E. García-España, S. Gama, S. Berto, D. Milea, PyES – an open-source software for the computation of solution and precipitation equilibria, *Chemom. Intell. Lab. Syst.* 239 (2023) 104860, <https://doi.org/10.1016/j.chemolab.2023.104860>.
- [35] A.W. Bauer, W.M. Kirby, J.C. Sherris, M. Turck, Antibiotic susceptibility testing by a standardized single disk method, *Am. J. Clin. Pathol.* 45 (1966) 493–496.
- [36] S.J. van Gerwen, F.M. Rombouts, K. van't Riet, M.H. Zwietering, A data analysis of the irradiation parameter D10 for bacteria and spores under various conditions, *J. Food Prot.* 62 (1999) 1024–1032, <https://doi.org/10.4315/0362-028x-62.9.1024>.
- [37] C. Sari, A comparative study of MTT and WST-1 assays in cytotoxicity analysis, *Haydarpassa Numune, Med. J.* (2019), <https://doi.org/10.14744/hnhj.2019.16443>.
- [38] F.S. Wahyuni, D.A. Israf Ali, N.H. Lajis, D. D. Anti-inflammatory activity of isolated compounds from the stem bark of *Garcinia cowa* Roxb, *Pharm. J.* 9 (2016) 55–57, <https://doi.org/10.5530/pj.2017.1.10>.
- [39] U.S.M. Rao, B. Ahmad, K. Mohd, *In vitro* nitric oxide scavenging and anti-inflammatory activities of different solvent extracts of various parts of *Musa paradisiaca*, *Malays. J. Anal. Sci* 20 (2016) 1191–1202.
- [40] A.E. Martell, R.M. Smith, R.J. Motekaitis, NIST Standard Reference Database 46, Gaithersburg, 2004.
- [41] L.D. Pettit, K.J. Powell. IUPAC Stability Constants Database, Academic Software, Otley, UK, 2004.
- [42] P.M. May, D. Rowland, K. Murray, E.F. May, Joint Expert Speciation System. http://jess.murdoch.edu.au/jess_home.htm, 2024 (accessed May 2024).
- [43] C.F. Baes, R.E. Mesmer, *The Hydrolysis of Cations*, Wiley, 1976.
- [44] C.F. Baes, R.E. Mesmer, The thermodynamics of cation hydrolysis, *Am. J. Sci.* 281 (1981) 935–962, <https://doi.org/10.2475/ajs.281.7.935>.
- [45] P.L. Brown, C. Ekberg, Aluminium, gallium, indium and thallium, hydrolysis of metal ions, John Wiley & Sons, Ltd, 2016, pp. 757–834.
- [46] R. Mladenova, T. Petrova, N. Manolova, M. Ignatova, I. Rashkov, P. Kubisa, Preparation, characterization, and biological activity of amides and esters from 8-Hydroxyquinoline-2-carboxylic acid and Jeffamines ED® or poly(ethylene glycol) S, *J. Bioact. Compat. Polym.* 16 (2001) 259–276, <https://doi.org/10.1106/AD9E-DQYK-579V-HT7A>.
- [47] L.G. Wade, J.W. Simek, *Organic Chemistry*, 9th edition, Pearson Education, India, 2020.
- [48] P.J. Linstrom, W.G. Mallard, NIST chemistry WebBook, NIST standard reference database number 69, National Institute of Standards and Technology. (2024), <https://doi.org/10.18434/T4D303>, 2024 (accessed May).
- [49] S. Cabo Verde, Food irradiation as sanitary treatment, in: I.C.F.R. Ferreira, A. L. Antonio, S. Cabo Verde (Eds.), *Food Irradiation Technologies: Concepts, Applications and Outcomes*, The Royal Society of Chemistry, 2017, pp. 183–209.
- [50] S. Gama, R. Hermenau, M. Frontauria, D. Milea, S. Sammartano, C. Hertweck, W. Plass, Iron coordination properties of Gramibactin as model for the new class of Diazeniumdiolate based Siderophores, *Chem. Eur. J.* 27 (2021) 2724–2733, <https://doi.org/10.1002/chem.202003842>.
- [51] F. Crea, C. De Stefano, C. Foti, D. Milea, S. Sammartano, Chelating agents for the sequestration of mercury(II) and monomethyl mercury(II), *Curr. Med. Chem.* 21 (2014) 3819–3836.